

Vibrations

Chapter Outline

- 5.1. Introduction 205
- 5.2. Theory 206
- 5.3. Global Ship Hull Vibrations 209
- 5.4. Vibrations of Local Structures 211
- 5.5. Effects of Adjacent Fluids: Hydrodynamic Mass 222
 - 5.5.1. Hydrodynamic Mass and Damping at Rudders 225
 - 5.5.2. Hydrodynamic Mass and Damping for Propellers 226
 - 5.5.3. Computation of Hydrodynamic Mass for Ships 227
 - 5.5.4. Damping of Ship Hull Vertical Vibrations 228
- 5.6. Excitation of Vibration 231
 - 5.6.1. Propellers 231
 - 5.6.2. Engine 232
 - 5.6.3. Seaway 233
 - 5.6.4. Vortex-Induced Vibrations 233
- 5.7. Effect of Vibrations 234
 - 5.7.1. Effects of Vibrations on the Ship 236
 - 5.7.2. Effects on Engines 237
 - 5.7.3. Effects of Vibrations on Humans 237

5.1. Introduction

Ship vibrations consider the ship hull and its structural members as *elastic* structures. Vibrations are important in the structural design due to the following design trends:

- Lightweight construction (with low stiffness and mass)
- Arrangement of living and working quarters near the propeller to optimize stowage space
- High propulsion power
- Small tip clearance of the propeller (to increase propeller efficiency)
- Fuel-efficient, slow-running main engines.

It has become standard practice to regulate vibration aspects for a newbuilding on a contractual basis. Therefore, vibration analyses are performed already during the preliminary or structural design stage for many ship types.

Vibrations cover the frequency range of 1 to 80 Hz according to ISO 6954. Table 5.1 shows typical natural frequencies of ship structures. Lower frequencies appear in ‘ship motions’ (classical ship seakeeping), higher frequencies in structure-borne noise (some overlap exists; noise may be perceived from 20 Hz upwards). Ship vibrations can become problematic if the exciting frequency is close to a natural frequency of the structure (resonance). Practical measures to avoid vibration problems include reduction of excitation amplitudes (e.g. elastic support for diesel engines) and avoidance of resonance at the lowest natural frequencies. As excitation frequencies of engines and propellers fluctuate with changing rpm, and natural frequencies of ship and some local structures (e.g. for tanks with various filling height) change with loading conditions, resonance at certain speeds often appears unavoidable.

Advances in computer methods have made many classical advanced beam models rather obsolete. Finite element analyses using rather large three-dimensional models are today standard tools, although simple beam theory allows understanding of certain typical relations and simple, fast (but often inaccurate) estimates.

5.2. Theory

Ship vibrations can generally be described by a linear equation of motion, allowing superposition of harmonic oscillations at different frequencies. The deflection (vector) $z(x)$ at point (vector) x of the vibrating structure follows then:

$$z(x, t) = \text{Re}[\hat{z}(x, t)e^{i\omega t}] \quad (5.1)$$

The circular frequency ω is connected to the frequency f by $\omega = 2\pi f$.

The motion equation for vibration problems contains the deflection and its first and second time derivatives:

$$K(z) + D(\dot{z}) + M(\ddot{z}) = F \quad (5.2)$$

Table 5.1: Natural frequency ranges in shipbuilding applications

	Min	Max
Global hull structures	0.5 Hz	10 Hz
Local structures	10.0 Hz	50 Hz
Deckhouse and aftbody structures	4.0 Hz	15 Hz
Structures above propeller	18.0 Hz	> 100 Hz
Large deck-panel structures	6.0 Hz	20 Hz
Engine foundations	20.0 Hz	> 100 Hz
Mast structures	7.0 Hz	21 Hz
Slow-running engines	4.5 Hz	12 Hz
Medium-speed engines, realistically supported	20.0 Hz	60 Hz
Medium-speed engines, mounted resiliently	1.5 Hz	7 Hz
Propeller shaft lines	4.0 Hz	19 Hz

$K(\ddot{z})$ is the stiffness operator, $D(\dot{z})$ the damping operator, and $M(\ddot{z})$ the mass operator, which may include added mass terms. $F(x, t)$ is the excitation force. For usually assumed harmonic excitation, we have:

$$F(x, t) = \text{Re}[\hat{F}(x)e^{i\omega t}] \quad (5.3)$$

For linear operators K , D , and M , we then have:

$$K(\hat{z}) + i\omega D(\hat{z}) - \omega^2 M(\hat{z}) = \hat{F}(x) \quad (5.4)$$

The natural frequency of a beam with flexible support on both ends (Fig. 5.1) is:

$$f = \frac{\pi}{2\ell^2} \sqrt{\frac{EI}{\rho A}} \quad (5.5)$$

Equation (5.5) can also be used to estimate the lowest natural frequency of a longitudinal stiffener (with plate) supported by many equidistant transverse large stiffeners. The transverse stiffeners increase both the stiffness of the support and the vibrating mass and the effects cancel each other largely, making the above formula applicable for each segment of such a continuous beam.

For a single beam, the next highest natural frequency appears for the natural mode of a full sinusoidal wave between the supports. The beam then vibrates as in lowest natural mode for half the beam length. The natural frequencies are thus four times as high. Generally the natural frequencies of the single beam on two supports increase as 1:4:9:16, etc. This is not the case for a continuous beam on equidistant supports (of distance ℓ). Here, higher natural modes can appear with more nodes in only one or several segments. Therefore the next highest natural frequencies of very long continuous beams are only a little higher than the lowest natural frequency and above the lowest natural frequency there is practically no resonance-free region.

A beam under compression close to the buckling limit will deflect largely even under minimum transverse load. Thus, such a beam has vanishing bending stiffness. Correspondingly its natural frequency will approach zero. For longitudinal stiffeners in ships, the natural frequency is thus changed depending on the global bending moments due to static (weight/buoyancy) and dynamic (seaway) bending moments, which induce compressive stresses particularly at the top deck or bottom of the ship.

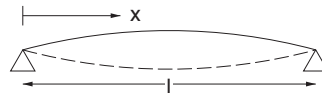


Figure 5.1:
Beam with flexible support on both ends

Consider a rectangular plane plate field (e.g. a plate between two longitudinal stiffeners and two transverse frames), considerably longer than wide (Fig. 5.2). Here the support from the longitudinal stiffeners (long side) is much stronger than the support from the transverse frames (short side). Each strip then vibrates almost like a beam with cross-section $b \cdot t$, where t is the plate thickness. However, unlike in a beam, the transverse contraction is suppressed by the adjacent strips. The effect is like an increased Young's modulus:

$$E^* = \frac{E}{1 - \nu^2} \quad (5.6)$$

The material constants for steel are $E = 2.1 \cdot 10^{11} \text{ N/m}^2$, $\rho = 7800 \text{ kg/m}^3$, $\nu = 0.3$. With $I = b \cdot t^3/12$ and $A = b \cdot t$, we then get the lowest natural frequency of a plate field:

$$f = \frac{\pi}{2 \cdot \ell^2} \cdot \sqrt{\frac{Et^2}{12\rho(1 - \nu^2)}} \quad (5.7)$$

The remarks concerning continuous beams and influence of compressive stress apply likewise for the case of continuous plate fields, but the effect is less pronounced.

Plate curvature influences stiffness. The effect depends on the support (boundary conditions). Example: A rectangular plate of side ratio 1:5, flexibly supported at all edges, vibrates in lowest natural mode (half wave in each direction) and has an initial deflection of the same form as the vibration mode. The lowest natural frequency is then increased as follows:

Deflection at plate center/plate thickness	0.25	0.50	0.75	1.00
Natural frequency increased by factor	1.04	1.15	1.30	1.50

In stiffened plate fields (with longitudinal and transverse stiffeners), one should then consider the following options to avoid resonance:

- vibration of plate fields, as treated above;
- vibration of the longitudinal stiffeners (modeling the transverse frames as supports), as treated above;

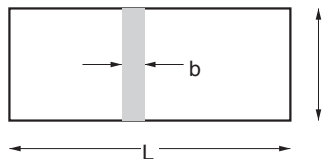


Figure 5.2:
Strip in a vibrating plate

- vibration of the transverse stiffeners. These are usually not slender enough to follow simple beam theory. Instead, bending and shear have to be considered together. Also, the support by the longitudinal stiffeners is usually too weak for the above simple models. More sophisticated analyses, typically employing finite element methods, are recommended.

The most important numerical techniques available to solve numerical vibration problems are:

- Finite element methods (FEM) approximate deflections by first-degree (for simple elements like trusses) and higher-order (for beams and plates) polynomials, typically Hermite polynomials.
- Spectral method, e.g. Doyle and Loh (1997): exact solutions are used for an idealized part of the structure, e.g. for a truss of constant section area.
- Rayleigh method, energy method: typically only one function is chosen to approximate the deflection, namely an estimated natural mode.

FEM are most popular, probably because the same software can be employed for static and vibration analysis, although spectral methods can be more efficient, particularly for higher frequencies.

5.3. Global Ship Hull Vibrations

The ship hull may perform global vibrations. The ship hull is usually (almost) symmetric to the centerplane in geometry and mass distribution. Then we can distinguish two types of natural modes:

- Vertical oscillations where points on the centerplane are displaced only within the centerplane. Vertical oscillations may induce significant longitudinal oscillations far away from the neutral layer (particularly on the bridge).
- Horizontal and torsional oscillations where points on the centerplane are displaced normal to the centerplane. For tankers, where the center of gravity and the shear center of cross-sections are close together, the horizontal vibrations are only weakly coupled to the torsional vibrations. Strong coupling is found in ships with large deck opening (container ships).

The lowest natural frequency for vertical vibrations appears for the two-node natural mode where two cross-sections remain (nearly) at rest. For a simple beam idealization, the next highest mode has three nodes (roughly twice the frequency), then four nodes (roughly three times the frequency), etc. A more detailed analysis shows further natural frequencies between these beam natural frequencies. These are due to local vibrations, e.g. of superstructures. The lowest natural frequency in vertical vibrations (two nodes) for ships of 150 m length lies typically around 1.5 Hz, for ships of 300 m length around 0.5 Hz. Because ships are typically wider than high, they are stiffer in the horizontal direction and the natural frequencies for horizontal vibrations are thus higher.

For a quick estimate, approximate formulae based on the simple beam models are useful. Lehmann (2000) gives for the lowest natural frequency (two nodes) for the steel ship hull girder in vertical bending:

$$f_0 = 1.62 \cdot 10^6 \cdot \sqrt{\frac{I}{\Delta_i \cdot L^3}} \quad (5.8)$$

The frequency is in Hz. I is the section moment of inertia amidships (m^4), Δ_i the displacement including a hydrodynamic mass (effect of surrounding water on vibrations) in kg:

$$\Delta_i = \left(1.2 + \frac{1}{3} \frac{B}{T}\right) \cdot \Delta \quad (5.9)$$

Δ is the mass of the ship (kg), L the ship length (m), B its width (m), T its draft (m).

For higher frequencies with n nodes we have:

$$f = (n - 1)^\mu \cdot f_0 \quad (5.10)$$

The exponent μ accounts for the effect of shear stiffness:

$$\mu = 1.02 \quad \text{for tankers;}$$

$$\mu = 1.0 \quad \text{for bulkers;}$$

$$\mu = 0.845 \quad \text{for cargo ships.}$$

These formulae cannot give more than a rough indication, particularly for the higher-order vibration modes.

Fast numerical computations of the ship hull vibrations employ beam models. The ship hull is then divided into beam segments. For each segment, mass per length, moments of inertia, etc. are taken as constant. The actual computation employs the method of transfer matrices. Vertical bending vibrations are relatively easy to analyze this way. They require ‘only’ the correct determination of bending stiffness and mass distribution. For horizontal vibrations, torsion and bending are strongly coupled, particularly for container ships. In practice, finite element programs are then employed, often using the services of classification societies.

The computations require longitudinal mass and stiffness distribution as input. The mass distribution considers the ship, the cargo and the hydrodynamic ‘added’ mass. The added mass reflects the effect of the surrounding water and depends on the frequency. Its determination is problematic. One can use estimates based on experience or employ sophisticated hydrodynamic simulations. Determination of the stiffness is also not trivial. Stress distributions in the stiffened bottom and deck plates depend on vibrational modes. Again either estimates based on experience or complex finite element analyses are employed. Estimates based on experience often work well. Of course the quality of the results depends on the input, which in

turn depends on experience. The large classification societies usually have enough experience to give good estimates for estimating stiffness and added mass.

If the hull is modeled in (relatively) great detail in a finite element analysis, the effective width does not have to be specified explicitly. Then the added mass matrix is best determined for all degrees of freedom using special potential flow codes. The finite element models have typically 20 000 to 40 000 degrees of freedom (Fig. 5.3). The primary structural components including large web frames are typically modeled using plane stress elements. The grids are not fine enough to reflect explicitly smaller structural details, such as stiffeners. If considered at all, these stiffeners are approximated by increasing the plate thickness. This reflects only the effect on the membrane stresses (in the plane of the plate), but not the change in bending stiffness. These models yield 50–150 vibration natural modes in the range up to 20 Hz (examples are given in Fig. 5.4). The container ship features particularly low natural frequencies in torsional vibrations due to large deck-opening (= low torsional stiffness). After the analysis, one then has to check whether the chosen model for the predicted natural modes is appropriate. Consideration of bending stiffness of the deck grillages in the finite element model requires representation of transverse and longitudinal deck girders at least in the form of beam elements. Such models have typically 40 000 to 80 000 degrees of freedom (Fig. 5.5), yielding 300 to 500 natural modes in the range up to 20 Hz (examples given in Fig. 5.6).

The preparation of the finite element input (elements, associated values, added masses) involves considerable experience and man-time (Fricke 2002), typically outsourced to special consultants or classification societies. Natural frequencies change with loading conditions. Typical loading conditions (mass distributions) should be selected rather than extreme conditions.

Despite the considerable effort, the employed finite element models are still not really satisfactory. Differences between computed and on-board measured vibration amplitudes by a factor of 3 are not uncommon. The reasons for this disappointing performance are not completely clear. One factor is modeling errors for curved shells, found particularly at the ship ends. The stiffness of these shells with respect to longitudinal bending depends very much on the arrangement of internal bulkheads and stiffeners, as well as the longitudinals between these transverse structural elements. These finer details of the structure are lost in the ‘coarse’ finite element grids typically employed.

5.4. Vibrations of Local Structures

Resonance problems often appear for local ship structures. This can affect human comfort, but also induce fatigue problems of structures. The vibration analysis of these local structures is similar to that for the ship hull and nowadays is often based on finite element methods.

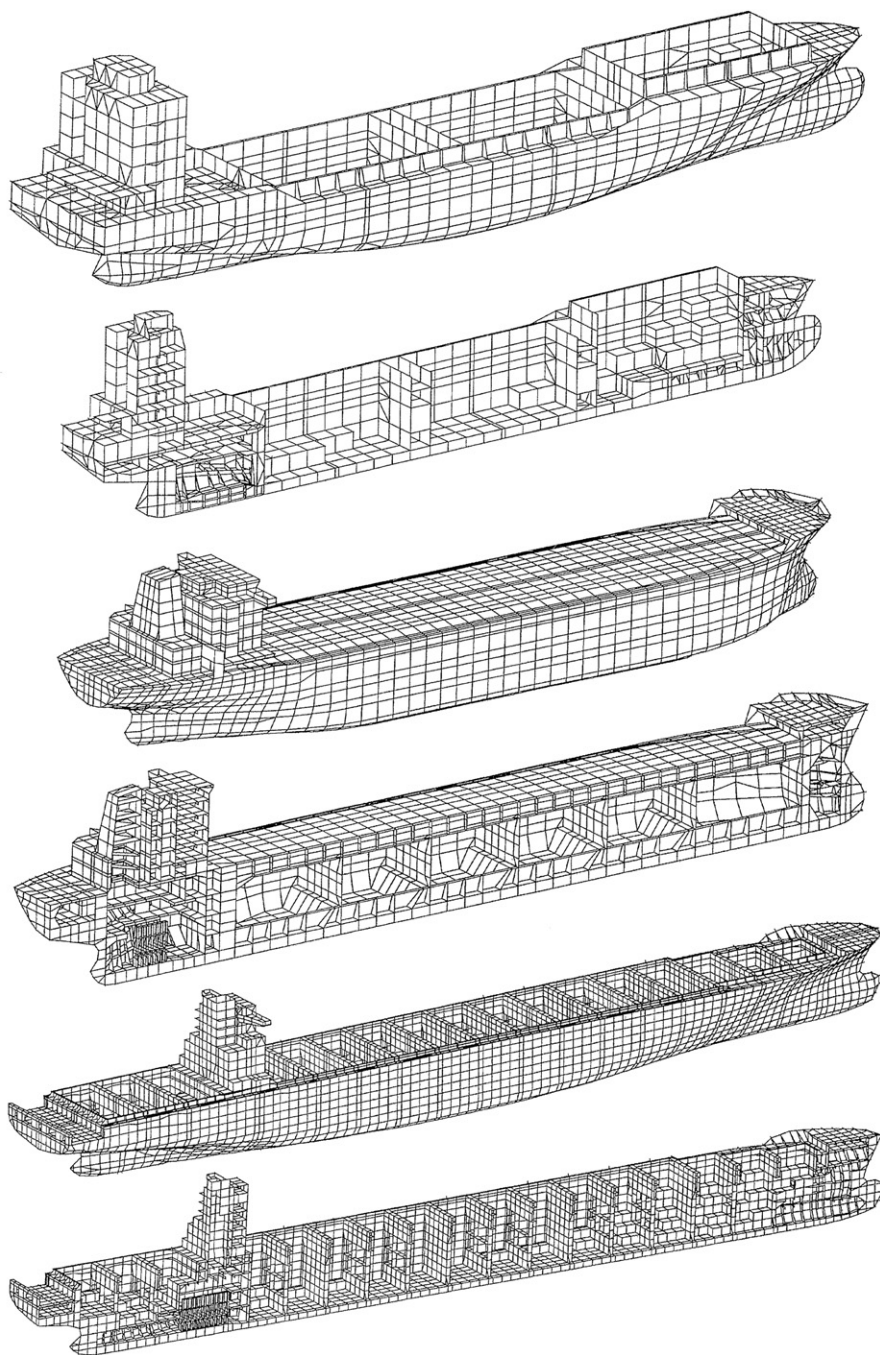


Figure 5.3:
FEM grids of some cargo ships. *Source: Germanischer Lloyd*

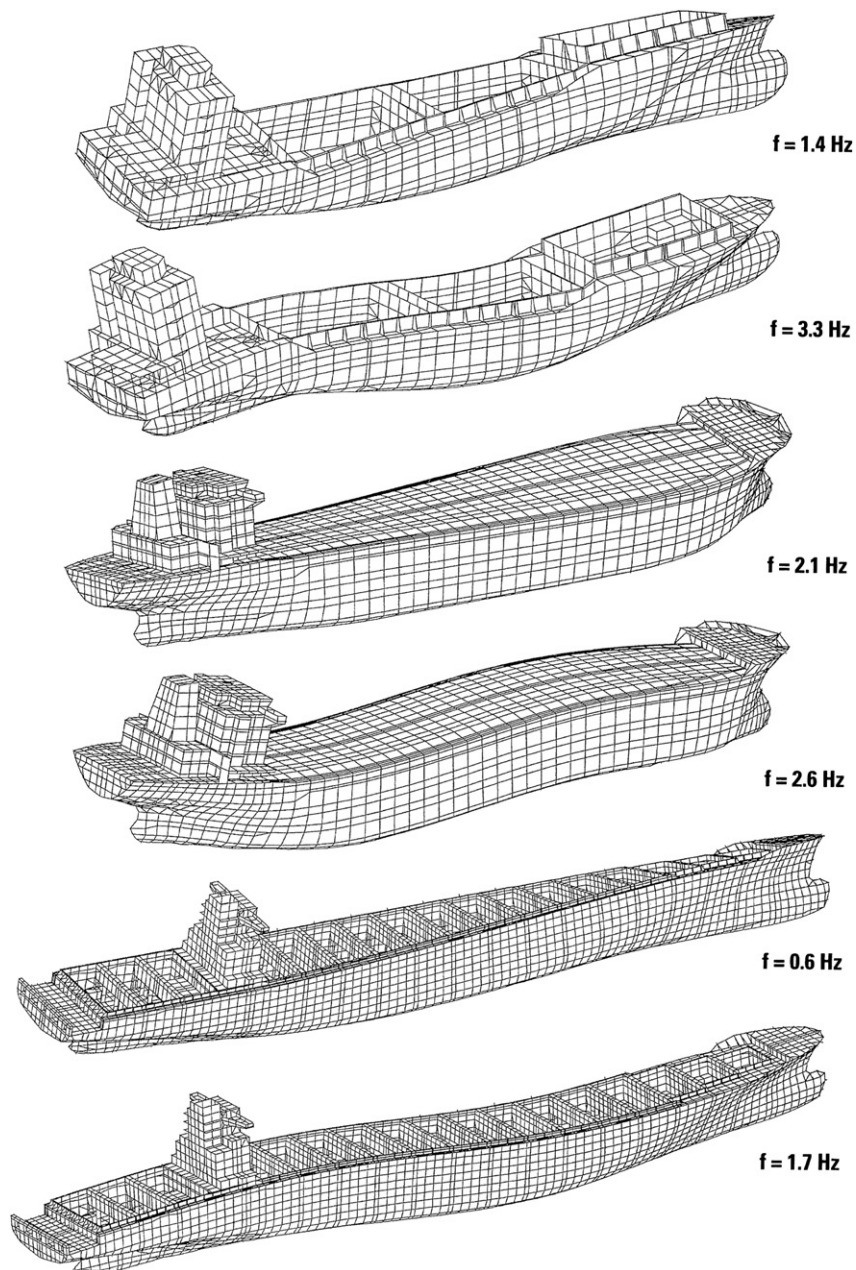


Figure 5.4:
Computed first torsional and second vertical vibration natural modes and corresponding natural frequencies for the ships in Fig. 5.3. *Source: Germanischer Lloyd*

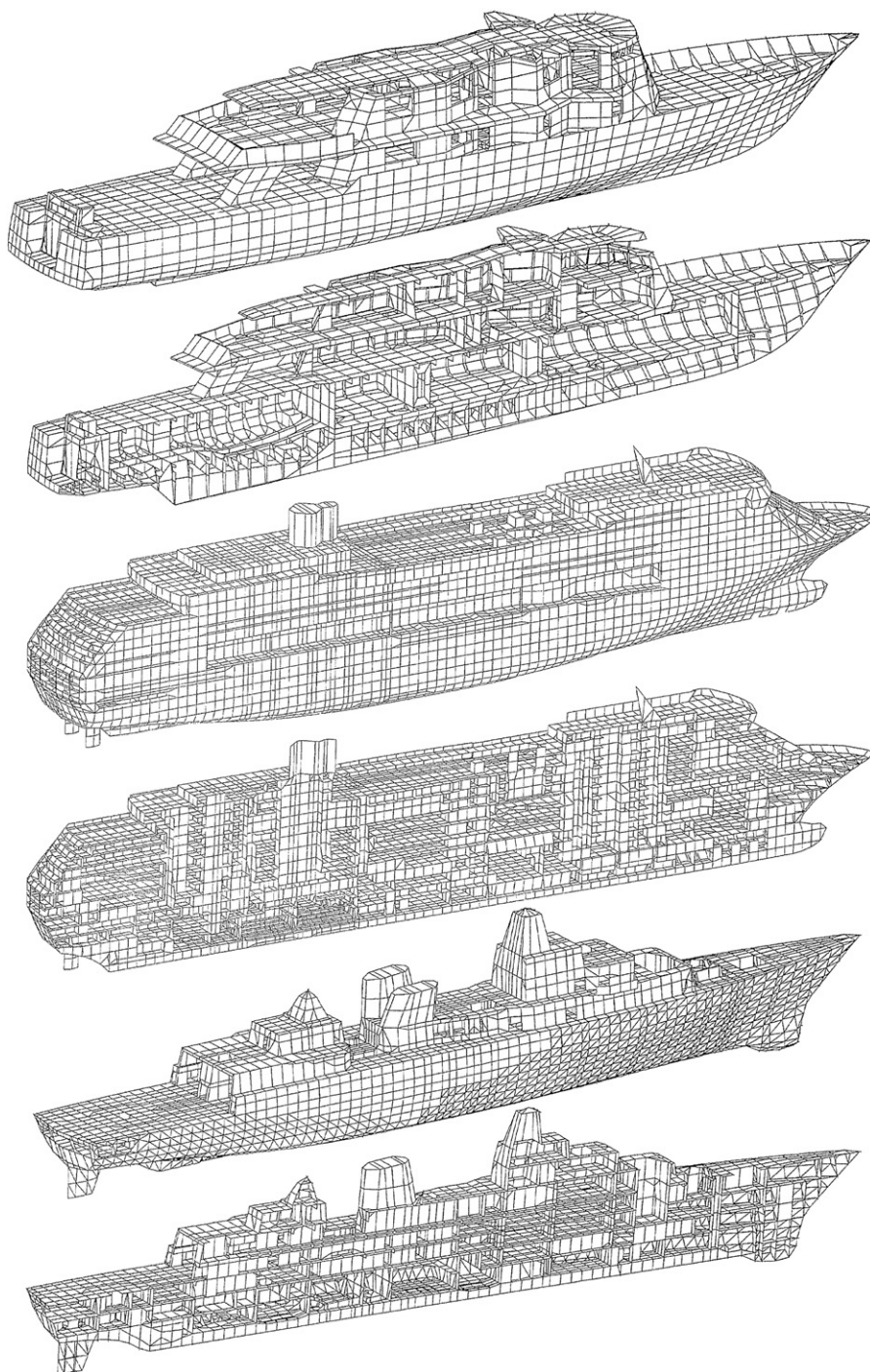


Figure 5.5:
FEM grids of a yacht, a passenger vessel, and a frigate. Source: *Germanischer Lloyd*

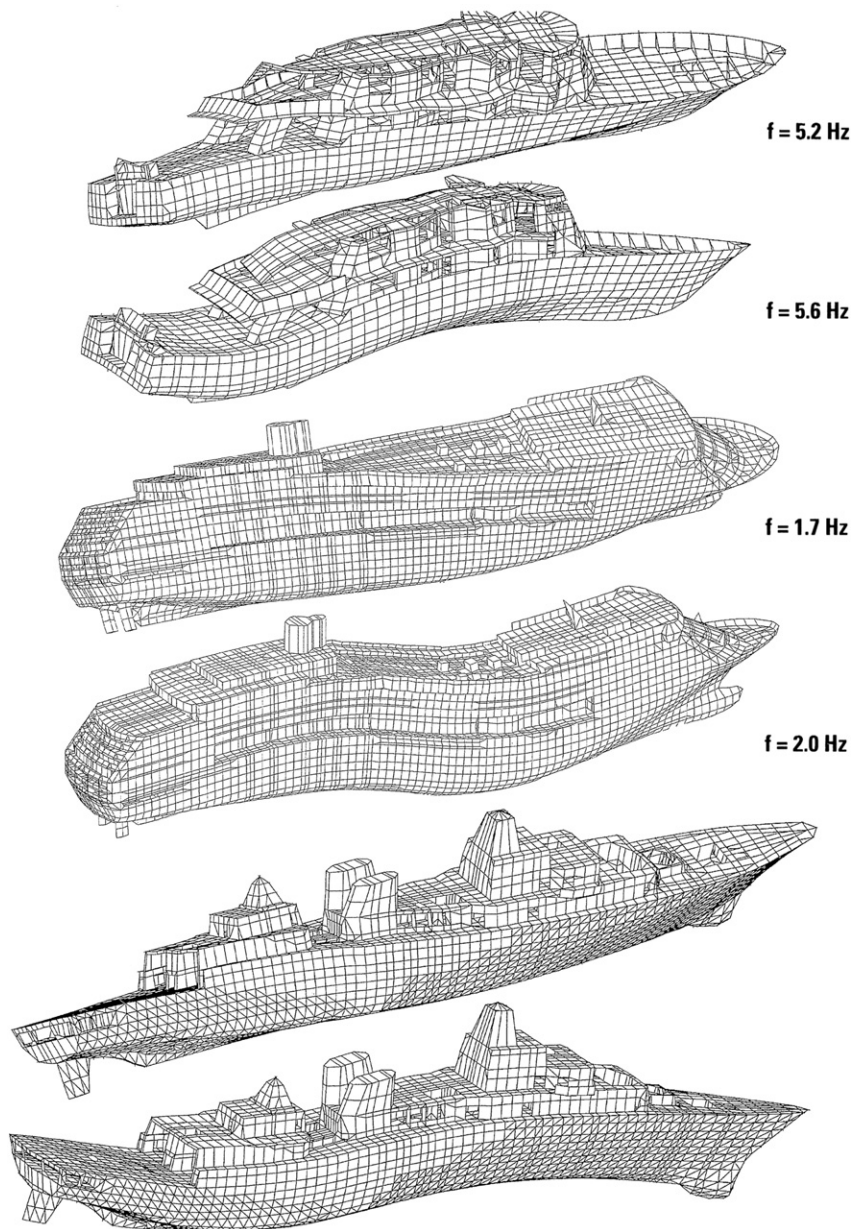


Figure 5.6:
Computed first torsional and second vertical vibration natural modes and corresponding natural frequencies for the ships in Fig. 5.5. Source: *Germanischer Lloyd*

For individual concentrated masses, the surrounding structure can be modeled in a single spring constant. The natural frequency of such a single mass-spring system is:

$$f = \frac{1}{2\pi} \sqrt{\frac{c}{m}} = \frac{1}{2\pi} \sqrt{\frac{g}{\delta_{\text{static}}}} \quad (5.11)$$

c is the spring constant, which follows from the static deflection of the system δ_{static} under a single mass load $m \cdot g$. Table 5.2 lists natural frequencies for several structures.

More often we have to consider distributed masses. The most common cases and corresponding natural modes and boundary conditions are listed in Table 5.3 with $\alpha = [\rho A / (EI)]^{-4} \sqrt{2\pi f}$ for a beam. For case 1 in Table 5.3, the (lowest) natural frequency is:

$$f_0 = \frac{\pi}{2\ell^2} \sqrt{\frac{EI}{\rho A}} \quad (5.12)$$

For all other boundary conditions we get $f = C \cdot f_0$. Table 5.4 compiles the constants C and natural modes. The free-free support yields the lowest natural frequencies. The lowest vibration mode and the next highest vibration mode are in this case rigid-body motions. The end supports influence the natural frequency. Figure 5.7 shows the natural frequency factor for a beam on two supports. The end support then varies from flexible ($\varepsilon = 0$) to fixed ($\varepsilon = 1$). The natural frequency is again given by $f = C \cdot f_0$. f_0 is the natural frequency of the beam with flexible end supports.

Some classification societies give approximate formulae to estimate the lowest natural frequencies of isotropic and orthotropic plate systems. These formulae often inherently assume partial support of the plate edges. The degree of support is often difficult to estimate, but influences the natural frequency. Generally, natural frequencies are given as functions of:

$$f \approx \left(\frac{1}{\ell^2}, \sqrt{\frac{I}{m}} \right) \quad (5.13)$$

Errors in estimating effective lengths between vibrational nodes propagate strongly (quadratic dependence on length). Errors in stiffness or mass are less important (square root dependence).

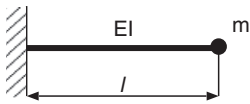
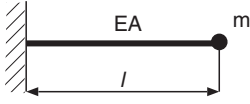
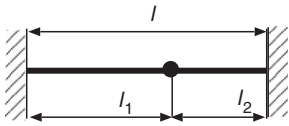
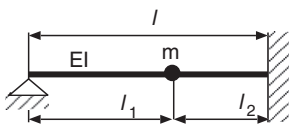
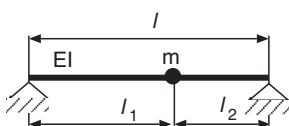
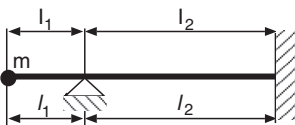
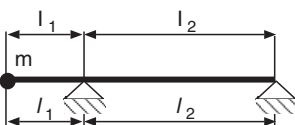
For the determination of the stiffness, it generally suffices to take an average plate width in the computations as follows:

$$B_m = 0.3 \cdot \ell \quad \text{for} \quad \ell/B \leq 3$$

$$B_m = B \quad \text{for} \quad \ell/B \geq 3$$

Here ℓ is the length between vibrational nodes. Stiffness and mass form a fraction. Thus errors usually cancel each other. Generally, accuracy decreases with higher vibrational modes. There is little sense in computing natural frequencies higher than the second or third harmonic.

Table 5.2: Natural frequencies f of typical structures (Lehmann 2000)

No.	System	Direction of vibration	Natural frequency
1		\updownarrow	$\frac{1}{2\pi} \sqrt{\frac{3EI}{\ell^3 m}}$
2		\leftrightarrow	$\frac{1}{2\pi} \sqrt{\frac{EA}{\ell \cdot m}}$
3		\updownarrow	$\frac{1}{2\pi} \sqrt{\frac{3EI\ell^3}{\ell_1^3 \cdot \ell_2^3 \cdot m}}$
4		\updownarrow	$\frac{1}{2\pi} \sqrt{\frac{4EI\ell^2}{\ell_1^2 \cdot \ell_2^3 \cdot \left[1 + \frac{\ell_1}{3\ell}\right] m}}$
5		\updownarrow	$\frac{1}{2\pi} \sqrt{\frac{3EI\ell}{\ell_1^2 \cdot \ell_2^2 \cdot m}}$
6	 $k = \frac{l_1 \ell_2}{l_2 \ell_1}$	\updownarrow	$\frac{1}{2\pi} \sqrt{\frac{12EI_1}{\ell_1^3 \cdot (4 + 3k) \cdot m}}$
7	 $k = \frac{l_1 \ell_2}{l_2 \ell_1}$	\updownarrow	$\frac{1}{2\pi} \sqrt{\frac{3EI_1}{\ell_1^3 \cdot (1 + k) \cdot m}}$

(Continued)

Table 5.2: Continued

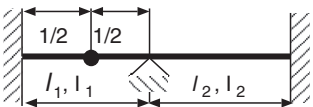
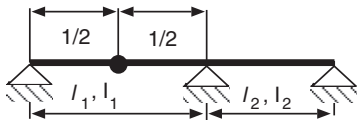
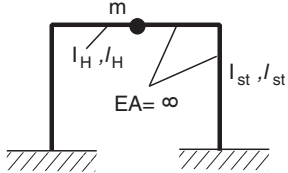
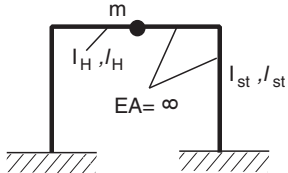
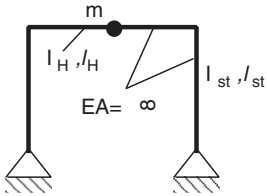
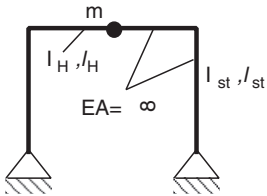
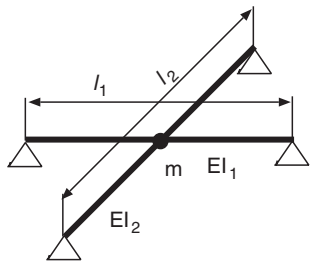
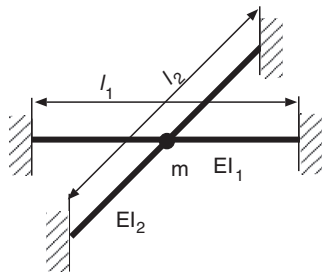
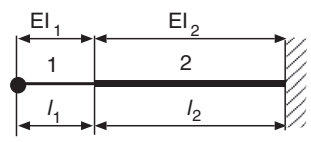
No.	System		Direction of vibration	Natural frequency
8		$k = \frac{I_1 \ell_2}{I_2 \ell_1}$	\updownarrow	$\frac{1}{2\pi} \sqrt{\frac{768 E I_1}{\ell_1^3 \cdot m} \cdot \left(\frac{k+1}{7k+4} \right)}$
9		$k = \frac{I_1 \ell_2}{I_2 \ell_1}$	\updownarrow	$\frac{1}{2\pi} \sqrt{\frac{768 E I_1}{\ell_1^3 \cdot m} \cdot \left(\frac{k+1}{16k+7} \right)}$
10		$k = \frac{I_H \ell_{St}}{I_{St} \ell_H}$	\updownarrow	$\frac{1}{2\pi} \sqrt{\frac{192 E I_H}{\ell_H^3 \cdot m} \cdot \left(\frac{k+2}{4k+2} \right)}$
11		$k = \frac{I_H \ell_{St}}{I_{St} \ell_H}$	\leftrightarrow	$\frac{1}{2\pi} \sqrt{\frac{24 E I_{St}}{\ell_{St}^3 \cdot m} \cdot \left(\frac{6k+1}{6k+4} \right)}$
12		$k = \frac{I_H \ell_{St}}{I_{St} \ell_H}$	\updownarrow	$\frac{1}{2\pi} \sqrt{\frac{192 E I_H}{\ell_H^3 \cdot m} \cdot \left(\frac{2k+3}{8k+3} \right)}$
13		$k = \frac{I_H \ell_{St}}{I_{St} \ell_H}$	\leftrightarrow	$\frac{1}{2\pi} \sqrt{\frac{6 E I_{St}}{\ell_{St}^3 \cdot m} \cdot \left(\frac{2k}{2k+1} \right)}$

Table 5.2: Continued

No.	System	Direction of vibration	Natural frequency
14	springs parallel: 	\updownarrow	$\frac{1}{2\pi} \sqrt{\frac{\delta_1 + \delta_2}{\delta_1 \delta_2}}$ $\delta_1 = \frac{\ell_1^3 m}{48EI_1}; \delta_2 = \frac{\ell_2^3 m}{48EI_2}$
15		\updownarrow	$\frac{1}{2\pi} \sqrt{\frac{\delta_1 + \delta_2}{\delta_1 \Delta_2}}$ $\delta_1 = \frac{\ell_1^3 m}{192EI_1}; \delta_2 = \frac{\ell_2^3 m}{192EI_2}$
16	springs sequential: 	\updownarrow	$\frac{1}{2\pi \sqrt{\delta_1 + \delta_2}}$ $\delta_1 = \frac{\ell_1^3 m}{3EI_1} \cdot \left(1 + 3 \frac{l_1 \ell_2}{l_2 \ell_1}\right);$ $\delta_2 = \frac{\ell_2^3 m}{3EI_2} \cdot \left(1 + 3 \frac{\ell_1}{\ell_2}\right)$


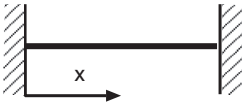
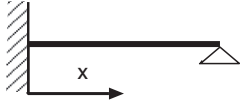
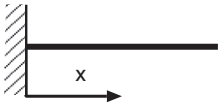
For vibrations of plates, we can use Fig. 5.8 to determine the lowest natural frequency for assorted side ratios and end supports with $f = C \cdot f_0$:

$$f_0 = \frac{\pi}{2b^2} \sqrt{\frac{Eh^2}{12(1-\nu^2)\rho}} \quad (5.14)$$

The simple formulae given above yield predictions which are good enough for practical purposes, provided that the following conditions are met (Asmussen et al. 1998):

- freely rotatable, fixed support at the edges;
- rectangular shape of grillage systems and plates;

Table 5.3: Natural modes for distributed mass systems (Lehmann 2000)

Case	System	Natural mode
1		$A \cdot \sin \alpha x$
2		$A \cdot \left[\sinh \alpha x - \sin \alpha x - \frac{\sinh \alpha \ell - \sin \alpha \ell}{\cosh \alpha \ell - \cos \alpha \ell} \cdot (\cosh \alpha x - \cos \alpha x) \right]$
3		$A \cdot [\sinh \alpha x - \sin \alpha x - \tan \alpha \ell \cdot (\cosh \alpha x - \cos \alpha x)]$
4		$A \cdot \left[\sinh \alpha x - \sin \alpha x - \frac{\sinh \alpha \ell - \sin \alpha \ell}{\cosh \alpha \ell - \cos \alpha \ell} \cdot (\cosh \alpha x - \cos \alpha x) \right]$

- regular arrangement of stiffeners;
- no pillars or stanchions within the considered system;
- uniform distribution of added mass.





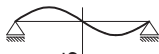


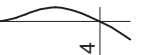




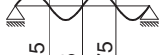


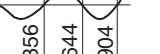




If these conditions are violated, finite element analyses must be employed. Because of the relatively high natural frequencies of local structures, the finite element models must be quite detailed, including also the bending stiffness of structural elements. The amount of work required for the creation of such models is considerable (and often underestimated) despite modern pre-processors with parameterized input possibilities and graphic support. Beam grillage models usually suffice for the lowest natural modes; for higher natural modes, three-dimensional models of higher precision are needed.

The distribution of effective masses in such models is often impossible to specify accurately. Asmussen et al. (1998), based on the experience of many vibration analyses for ship structures at Germanischer Lloyd, recommend taking an effective additional mass of 40 kg/m^2 into account for decks in living and working spaces and 20 kg/m^2 for bulkheads.

Ideally, ship structures have natural frequencies (well) above the main exciting frequencies (subcritical design). Asmussen et al. (1998) give as guidelines:

- natural frequency greater than 1.2 times, twice the propeller blade frequency or main engine ignition frequency in the ship's aftbody, engine room, and deckhouse area;

Table 5.4: Natural modes and natural frequency for beams (Lehmann 2000)

	1	2	3	4
				
	$\frac{f}{f_0} = 1.0$	$\frac{f}{f_0} = 2.267$	$\frac{f}{f_0} = 1.562$	$\frac{f}{f_0} = 0.356$
1. higher	 0.5	 0.5	 0.588	 0.744
	$\frac{f}{f_0} = 4.0$	$\frac{f}{f_0} = 6.259$	$\frac{f}{f_0} = 5.07$	$\frac{f}{f_0} = 1.562$
2. higher	 0.333 0.667	 0.359 0.641	 0.385 0.691	 0.5 0.868
	$\frac{f}{f_0} = 9.0$	$\frac{f}{f_0} = 12.241$	$\frac{f}{f_0} = 10.78$	$\frac{f}{f_0} = 6.259$
3. higher	 0.25 0.5 0.75	 0.278 0.5 0.722	 0.296 0.526 0.766	 0.356 0.644 0.904
	$\frac{f}{f_0} = 16.0$	$\frac{f}{f_0} = 20.244$	$\frac{f}{f_0} = 18.05$	$\frac{f}{f_0} = 12.24$
4. higher	 0.2 0.4 0.6 0.8	 0.227 0.409 0.591 0.773	 0.239 0.429 0.616 0.81	 0.279 0.5 0.723 0.926
	$\frac{f}{f_0} = 25.0$	$\frac{f}{f_0} = 30.15$	$\frac{f}{f_0} = 27.59$	$\frac{f}{f_0} = 20.244$

- natural frequency greater than 1.1 times the propeller blade frequency for the ship's shell structure directly above the propeller.

The assumption of simply supported edges is conservative, as any constraining effect increases the natural frequency further. To avoid in turn over-dimensioning, stiff bracket connections are sometimes considered by taking 50–70% of the bracket length as 'effective', reducing correspondingly the lengths of beam elements.

In most cases, it is sufficient to design natural frequencies of local structures subcritically up to 35 Hz. Further increases of natural frequencies usually come at exhibitive cost. A supercritical design (natural frequency (well) below exciting frequency) or a 'design in frequency windows' (between exciting frequencies) is then chosen for such high frequencies.

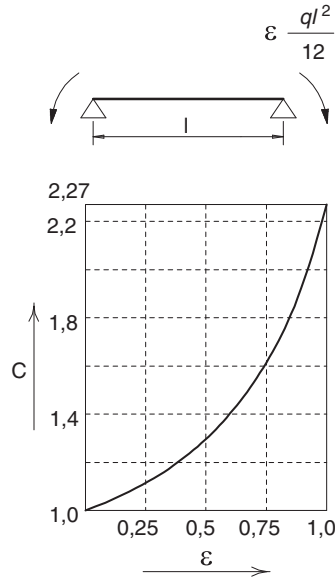


Figure 5.7:
Beam on two supports (from flexible to fixed)

5.5. Effects of Adjacent Fluids: Hydrodynamic Mass

Ship structures often border water or other fluids (e.g. fuel), either on one side (outer hull plates) or both sides (fuel tank bulkhead). Fluid immersion can be total or partial. If the structure borders a fluid, structure vibrations will induce fluid motions. This induces a pressure from the fluid to the structure.

The effect of adjacent fluids on the mass operator is usually large, its effect on damping and stiffness small. The small effect on damping can nevertheless be important, because other damping mechanisms are also small. Changes in displacement volume (increased or decreased immersion) affect the stiffness operator (restoring forces). The ‘hydrostatic stiffness’ increases the natural frequency of vertical bending vibrations of the hull girder. The effect is usually negligible, except perhaps for particularly ‘soft’ ships such as inland cargo vessels.

In the following we discuss the influence on the mass operator. The ‘added mass’ or ‘hydrodynamic mass’ is the equivalent mass one would have to fix to the structure to obtain the same effect on the structure as the adjacent accelerated fluid has.

The fundamental equation for the hydrodynamic mass A is:

$$A = \sum_S \int \frac{1}{\omega^2} p_a \cdot \vec{n} \cdot \vec{q}_j \, dS \quad (5.15)$$

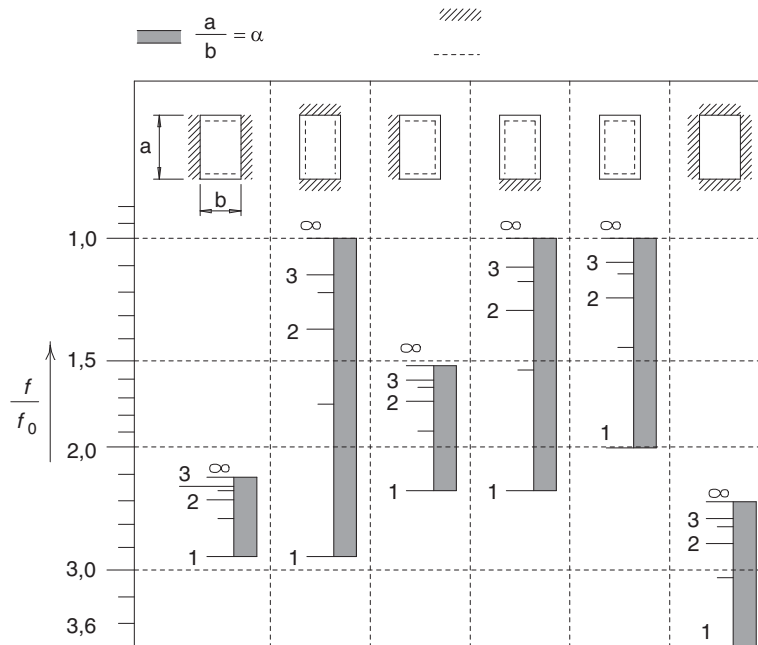


Figure 5.8:

Natural frequencies of rectangular plates; //// fixed support, - - - flexible support (Lehmann 2000)

\vec{n} is the unit normal pointing from the fluid to the body, \vec{q}_j the j^{th} deflection form, and p_a the amplitude of the oscillating part of the pressure (due to a certain natural mode).

For an infinite plate with the fluid of density ρ above the plate (Fig. 5.9) the added mass for a plate strip of length a and width b orthogonal to the paper plane is:

$$A = \frac{\rho a^2 b}{\pi} \quad (5.16)$$

The formula is valid for infinite plate extension with all plate segments vibrating sinusoidally and no obstacles in the flow. The formula is based on potential flow considerations. Viscosity generally plays a negligible role in plate vibrations in ships. For typical ship plates covered by water or fluids of similar density (like oil), the added mass exceeds the structural mass.

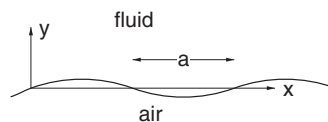


Figure 5.9:

Plate with adjacent fluid on one side

For example, for a 10-mm steel plate and distance between nodes 700 mm, the steel mass per area is $7.8 \text{ t/m}^3 \cdot 0.01 \text{ m} = 0.078 \text{ t/m}^2$; the added mass due to fresh water on one side is already $1 \text{ t/m}^3 \cdot 0.7 \text{ m} / \pi = 0.223 \text{ t/m}^2$. If the plate has water on both sides, the added mass value doubles. For larger stiffened plate areas which oscillate including their stiffeners, the added mass effect dominates even more.

Equation (5.7) for a plate vibrating in air is now modified for adjacent fluids:

$$f = \frac{\pi}{2 \cdot \ell^2} \cdot \sqrt{\frac{Et^3}{12(1 - \nu^2)(\rho_{st} \cdot t + \rho_f \cdot \ell / \pi)}} \quad \text{for fluid on one side} \quad (5.17)$$

$$f = \frac{\pi}{2 \cdot \ell^2} \cdot \sqrt{\frac{Et^3}{12(1 - \nu^2)(\rho_{st} \cdot t + 2\rho_f \cdot \ell / \pi)}} \quad \text{for fluid on both sides} \quad (5.18)$$

ρ_{st} is the density of the structure, ρ_f the density of the adjacent fluid, ℓ the length between nodes (plate length in lowest frequency mode = spacing of stiffeners), and t the plate thickness.

Various factors may in practice change the effect of adjacent fluids and thus the natural frequency of ship plates. Generally, each constraint of fluid motion increases the added mass, each relaxation (e.g. due to three-dimensional effects) decreases the added mass. In particular:

- Rectangular plates (limited side ratio)

The previous formulae for plates assumed large side ratio ($a \ll b$). For the general case, the lowest natural frequency is:

$$f = \left(\frac{\pi}{2 \cdot a^2} + \frac{\pi}{2 \cdot b^2} \right) \sqrt{\frac{Et^3}{12(1 - \nu^2)(\rho_{st} \cdot t + \rho_f \cdot d)}} \quad (5.19)$$

d is the thickness of an equivalent ‘water layer’ (a mass layer attached to the structure giving the same mass effect as the added mass). In this case:

$$d = \frac{1}{\pi \sqrt{a^{-2} + b^{-2}}} \quad (5.20)$$

- A rigid wall at distance h parallel to the vibrating plate modifies d by a factor:

$$\frac{1}{\tanh(\pi h \sqrt{a^{-2} + b^{-2}})} \quad (5.21)$$

- A constant flow parallel to the plate with speed V (hull plating neglecting boundary layer) modifies d by the factor $1 + \left(\frac{V\pi}{\omega a'} \right)^2$. a' is the distance between vibration nodes in the flow direction.

- Vibrating plate between rigid walls orthogonal to the plate
The added mass becomes very large, unless the plate moves in a vibration mode keeping the fluid volume constant (i.e. lowest natural mode is full sine wave between nodes). This case appears typically for tank walls. As a consequence of these natural modes, the added masses are much lower.
- Plate curvature (shells)
Plate curvature decreases/increases added mass if the fluid is on the convex/concave side. The effect is usually small.
- Perforated plates
If the structure is perforated, the added mass is reduced by multiplying the added mass of the full plate by a reduction factor, which can be simply approximated following Lehmann (2000):

$$C_{\text{red}} = 1 - 8.44\alpha + 27.6\alpha^2 - 30.2\alpha^3, \text{ where } \alpha \text{ is the ratio of area of hole/area of the plate.}$$

5.5.1. Hydrodynamic Mass and Damping at Rudders

We consider first the two-dimensional case (infinite rudder height) in uniform flow of speed U . The rudder makes harmonic transverse motions q_1 and rotational motions q_2 around the center of the chord (Fig. 5.10).

Let the non-dimensional frequency be $\pi \cdot f \cdot c / U > 2$. Then the transverse force F_1 and the transverse F_2 (around the point on half chord length) are almost the same as for infinite frequency. The hydrodynamic force vector is then expressed as usual, with components proportional to accelerations, velocities, and deflections:

$$\begin{Bmatrix} F_1 \\ F_2 \end{Bmatrix} = -A \begin{Bmatrix} \ddot{q}_1 \\ \ddot{q}_2 \end{Bmatrix} - D' \begin{Bmatrix} \dot{q}_1 \\ \dot{q}_2 \end{Bmatrix} - K'' \begin{Bmatrix} q_1 \\ q_2 \end{Bmatrix} \quad (5.22)$$

The hydrodynamic stiffness matrix K'' is negligibly small in comparison to the structural stiffness. Added mass and damping matrices are:

$$A = \begin{bmatrix} \pi \rho_f c^2 / 4 & 0 \\ 0 & \pi \rho_f c^4 / 128 \end{bmatrix} \quad \text{and} \quad D' = \begin{bmatrix} \pi \rho_f c |U| / 2 & 3\pi \rho_f c^2 |U| / 8 \\ -\pi \rho_f c^2 |U| / 8 & \pi \rho_f c^3 |U| / 32 \end{bmatrix} \quad (5.23)$$

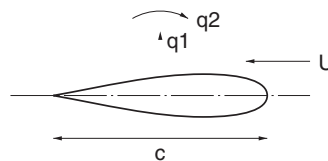


Figure 5.10:
Notation for rudder

For three-dimensional flow (finite rudder height h), the top left element of the added mass matrix is reduced by a factor as follows:

h/c	10	5	4	2.5	2	1.5	1	0.5
Reduction factor	0.94	0.90	0.87	0.80	0.76	0.70	0.48	0.38

Reduction factors for other matrix elements are not known. If required they should be determined by more elaborate numerical simulations. If the coordinate system is not at half chord length, but shifted upstream by a distance e (e.g. at the center of the profile area), we have (neglecting the small hydrodynamic stiffness):

$$\begin{Bmatrix} F_1 \\ F_2 \end{Bmatrix}_{\text{w.r.t. } e} = - \begin{bmatrix} 1 & 0 \\ e & 1 \end{bmatrix} M \begin{bmatrix} 1 & e \\ 0 & 1 \end{bmatrix} \begin{Bmatrix} \ddot{q}_1 \\ \ddot{q}_2 \end{Bmatrix}_{\text{w.r.t. } e} - \begin{bmatrix} 1 & 0 \\ e & 1 \end{bmatrix} D \begin{bmatrix} 1 & e \\ 0 & 1 \end{bmatrix} \begin{Bmatrix} \dot{q}_1 \\ \dot{q}_2 \end{Bmatrix}_{\text{w.r.t. } e} \quad (5.24)$$

5.5.2. Hydrodynamic Mass and Damping for Propellers

Schwanecke (1963) used an unsteady lifting-line method to compute mass and damping matrices for propellers vibrating in six degrees of freedom as rigid bodies. x points forward, y to port, z upward. Then forces and moments are expressed as:

$$\begin{Bmatrix} F_x \\ M_x \\ F_y \\ M_y \\ F_z \\ M_z \end{Bmatrix} = - \begin{bmatrix} a_{11} & a_{12} & 0 & 0 & 0 & 0 \\ a_{12} & a_{22} & 0 & 0 & 0 & 0 \\ 0 & 0 & a_{33} & a_{34} & 0 & 0 \\ 0 & 0 & a_{34} & a_{44} & 0 & 0 \\ 0 & 0 & 0 & 0 & a_{33} & a_{34} \\ 0 & 0 & 0 & 0 & a_{34} & a_{44} \end{bmatrix} \begin{Bmatrix} \ddot{u}_x \\ \ddot{\alpha}_x \\ \ddot{u}_y \\ \ddot{\alpha}_y \\ \ddot{u}_z \\ \ddot{\alpha}_z \end{Bmatrix} - \begin{bmatrix} b_{11} & b_{12} & 0 & 0 & 0 & 0 \\ b_{12} & b_{22} & 0 & 0 & 0 & 0 \\ 0 & 0 & b_{33} & b_{34} & b_{35} & b_{36} \\ 0 & 0 & b_{34} & b_{44} & b_{45} & b_{46} \\ 0 & 0 & -b_{35} & -b_{36} & b_{33} & b_{34} \\ 0 & 0 & -b_{45} & -b_{46} & b_{34} & b_{44} \end{bmatrix} \begin{Bmatrix} \dot{u}_x \\ \dot{\alpha}_x \\ \dot{u}_y \\ \dot{\alpha}_y \\ \dot{u}_z \\ \dot{\alpha}_z \end{Bmatrix} \quad (5.25)$$

u denotes deflections, α rotations. Schwanecke approximates the elements of the mass and damping matrices as functions of area ratio A_E/A_0 , propeller pitch P , blade number Z , diameter D , and propeller circular frequency ω_w :

$$a_{11} = 0.209 \pi \rho D^3 (A_E/A_0)^2 / Z \quad a_{12} = -0.105 \rho D^4 (P/D) (A_E/A_0)^2 / Z$$

$$\begin{aligned}
a_{22} &= 0.052 \rho D^5 (P/D)^2 (A_E/A_0)^2 / (\pi Z) & a_{33} &= 0.566 \rho D^3 (P/D)^2 (A_E/A_0)^2 / (\pi Z) \\
a_{34} &= 0.052 \rho D^4 (P/D) (A_E/A_0)^2 / Z & a_{44} &= 0.009 \pi \rho D^5 (A_E/A_0)^2 / Z \\
b_{11} &= 0.066 \pi \rho \omega_w D^3 (A_E/A_0) & b_{12} &= -0.033 \rho \omega_w D^4 (A_E/A_0) \\
b_{22} &= 0.017 \rho \omega_w D^5 (P/D)^2 (A_E/A_0) / \pi & b_{33} &= 0.124 \rho \omega_w D^3 (P/D)^2 (A_E/A_0) / \pi \\
b_{44} &= 0.004 \pi \rho \omega_w D^5 (A_E/A_0) & b_{34} &= 0.017 \rho \omega_w D^4 (P/D) (A_E/A_0) \\
b_{35} &= 0.566 \rho \omega_w D^3 (P/D)^2 (A_E/A_0)^2 / (\pi Z) & b_{36} &= 0.105 \rho \omega_w D^4 (P/D) (A_E/A_0)^2 / Z \\
b_{45} &= 0.052 \rho \omega_w D^4 (P/D) (A_E/A_0)^2 / Z & b_{46} &= 0.017 \pi \rho \omega_w D^5 (A_E/A_0)^2 / Z
\end{aligned}$$

5.5.3. Computation of Hydrodynamic Mass for Ships

Because ships are longitudinal, slender structures, we assume (approximately) that the water flows around individual strips (rather than in the x direction). This assumption for the ship vibrations is the same as for the rigid-body motions of the ship in ship seakeeping.

Lewis (1929) already computed the motion of water around vertically oscillating ship cross-sections using conformal mapping for the limiting case of infinite frequency. This approximation is already sufficiently accurate for the lowest vibration natural mode with two nodes. In this case, the free-surface water motion is limited to a vertical motion. (However, for lower frequencies as in rigid-body ship seakeeping, we should also consider the horizontal water motion in a more sophisticated model.) The result of the Lewis approach can be summarized as follows. The added mass (per length) of a cross-section is:

$$m''_{33} = \rho \cdot \frac{\pi}{2} r^2 [(1-a)^2 + 3b^2] \quad (5.26)$$

ρ is the water density. The three parameters r , a , and b characterize size and shape of the cross-section. They follow from the following non-linear system of equations:

$$\frac{B}{2T} = \frac{1-a+b}{1+a+b} \quad (5.27)$$

$$C_M = \frac{\pi}{4} \frac{1-a^2-3b^2}{(1+b)^2-a^2} \quad (5.28)$$

$$r = \frac{B}{2(1-a+b)} \quad (5.29)$$

B is the cross-section width in the waterline, T its draft (at $y = 0$), and C_M its cross-section coefficient = cross-section area/($B \cdot T$). This system of equations has two solutions. The

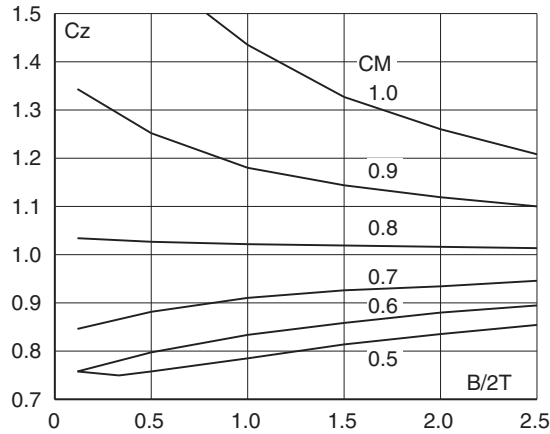


Figure 5.11:

Coefficient of hydrodynamic mass of ship cross-section $C_z = m''/(\rho\pi B^2/8)$ for high-frequency vertical motion at the water surface

resulting minimum added mass m'' is taken. Figure 5.11 shows results for a non-dimensional coefficient of the added mass.

For high-frequency horizontal vibrations of a cross-section at a free surface, the hydrodynamic mass (per length) is almost independent of the cross-section shape:

$$m''_{22} = 0.205\pi\rho T^2 \quad (5.30)$$

The hydrodynamic mass for roll motion can be approximated for a surface piercing cross-section:

$$m''_{44} = \left[1 - \left(\frac{2T}{B}\right)^2\right]^2 \cdot \pi \frac{\rho B^4}{256} \quad (5.31)$$

For submerged cross-sections near the free surface, this value needs to be doubled. For cross-sections with sharp bilge corners or bilge keels, the hydrodynamic added mass can be considerably larger.

All these values are for two-dimensional strips, assuming that the water moves only in the plane of the strip. This assumption is increasingly less valid as the distance between vibration nodes decreases with respect to strip width (for vertical and torsional vibrations) and draft (for horizontal vibrations). Figure 5.12 gives necessary reduction factors J to account for three-dimensional effects. These curves were determined numerically by a boundary element method.

5.5.4. Damping of Ship Hull Vertical Vibrations

Numerical (deformation) methods compute the vertical vibrations of the ship hull using mass, damping, and stiffness matrices. The damping matrix is generally expressed as follows:

$$D_{ij} = \int_L d(x) \cdot q_i(x) \cdot q_j(x) \, dx \quad (5.32)$$

$d(x)$ is the damping force per length, divided by the vertical velocity of the cross-section. q_i and q_j are the shape functions for the vertical deflections of the ship cross-sections.

If we use the vibration natural modes for q_i , the mass matrix and the stiffness matrix are simple diagonal matrices. The damping of vertical ship hull vibrations is weak. Therefore, the off-diagonal elements in the damping matrix can be neglected and the individual vibration modes can be considered separately.

We can estimate the hydrodynamic damping as follows:

$$D_{ii} = \int_L \left(q_i^2 + \frac{U^2}{\omega^2} (q_i')^2 \right) N \, dx + \rho \int_L c_w B |w| q_i^2 \, dx \quad (5.33)$$

$$+ \frac{U^2}{\omega^2} q_{iT} q_{iT}' N_T + U q_{iT}^2 m_T'' + \frac{\rho}{4} n D_P P^2 q_{iP}^2$$

The first term is due to the waves radiated from the vibrating hull and can be computed in a strip method as for the rigid-body motions. U is the ship speed and q_i' the derivative of the shape function (natural mode) with respect to x . $N(x)$ is the damping constant (per length) for a given strip. N depends on section shape and frequency. For high-frequency

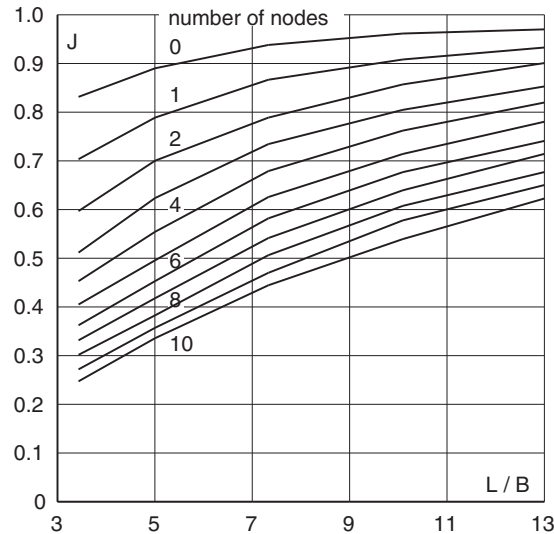


Figure 5.12:

Reduction factor J for hydrodynamic masses for three-dimensional flow in vertical ship vibrations

radiated waves (with wave lengths much shorter than the section width), we can approximate:

$$N(x) \approx \rho \frac{gB(x)\tan \alpha}{2\omega} \quad (5.34)$$

$B(x)$ is the local section width and α the flare angle in the waterline measured against the vertical ($\alpha = 0^\circ$, i.e. $N = 0$, for wall-sided sections).

The second term is due to the pressure resistance of the vertically moving cross-sections. The contribution of the vibrations by themselves is negligibly small, but the interaction with rigid-body motions is considered here by the average vertical velocity $|w|$. c_w is the vertical motion resistance coefficient of the section. Lacking better data, one employs here steady flow resistance values, typically $0.5 < c_w < 1$ for the midbody sections. At the ship ends, where the sections are well-rounded, c_w is negligibly small.

The third and fourth terms consider the effect of the transom stern (thus index T , e.g. $q_{iT} = q_i(x_T)$ is the value of the shape function at the transom). N_T is the damping constant, m_T'' the added mass, both for high-frequency and the transom shape. These terms assume a detaching flow at the transom, similar to that in the strip method. Note that the wetted transom stern in operation (with ship wave system and motions in seaways) differs from that at rest. The third term containing N_T is typically much smaller than the fourth term and can usually be neglected.

The last term is due to the propeller. q_{iP} is the value of the shape function at the propeller, D_P the propeller diameter, P the propeller pitch, and n the propeller revolutions (in 1/s).

The terms depend on ship speed, motions in seaways and propeller actions. Therefore vibration damping in port will be different from actual operation conditions.

Besides hydrodynamic damping, material damping and component damping (due to floor and deck coverings) play a role in damping. In the literature, widely different values are stated for damping characteristics and the uncertainty increases for higher frequencies. For simple practical estimates, Asmussen et al. (1998) give:

- for ship in loaded condition: $\vartheta = \min(8; 7 \cdot f/20 + 1)\%$
- for ship in ballast condition: $\vartheta = \min(6; 5.5 \cdot f/20 + 0.5)\%$

The frequency f is taken in Hz. The degree of damping ϑ is coupled to the logarithmic decrement Λ :

$$\Lambda = \frac{2\pi \cdot \vartheta}{\sqrt{1 - \vartheta^2}} \quad (5.35)$$

The logarithmic decrement describes the ratio of two successive maxima: $e^\Lambda = A_1/A_2$.

5.6. Excitation of Vibration

Ship hull vibrations are mainly excited by seaway, propeller, and main engines. In addition there are special cases, where periodic flow separation at structure appendages or torque fluctuations in electric engines excite structural vibrations, for example.

5.6.1. Propellers

Propellers excite vibrations by induced pressure fluctuations on the ship hull and on the rudder. The propeller induces a pressure field, due to the displacement effect of the propeller blades and due to the changing cavitation volume on cavitating propellers. The contribution due to cavitation is often more important for vibration excitation. The exciting frequencies of a propeller are generally $\text{rpm} \times \text{number of blades}$ and higher harmonics. Thus we have, say, for a four-bladed propeller with $120 \text{ rpm} = 2 \text{ Hz}$: 8, 16, 24, ... Hz as exciting frequencies. In choosing an appropriate number of propeller blades, one tries to place the propeller excitation in an interval between hull natural frequencies. For modern propellers, excited pressure impulses at second, third, or fourth blade frequency are typically higher than at blade frequency. The explanation is that modern numerical propeller design tools (panel methods) allow the cavitation volume on the propeller responsible for pressure fluctuations at blade frequency to be relatively well minimized. Higher-frequency excitations are largely due to tip-vortex cavitation. Scale effects play a more significant role for higher-order excitations. Holden et al. (1980) give empirical formulae to estimate the cavitation-induced pressure on the ship hull of single-screw ships, but numerical methods (panel methods or lifting surface methods) are state-of-the-art to numerically predict induced pressure fluctuations. RANSE methods including cavitation models drift increasingly into industrial applications. Still, numerical simulations in the initial design phase are usually followed by model tests, using facilities that allow high Reynolds numbers. Model tests can measure pressure impulses on the hull. For simpler tests, the ship wake is approximated using a fine grid upstream and the pressure impulses are measured on a flat plate above the propeller approximately at a position where in reality the ship hull is. For tests with complete ship models, a grid of pressure probes is installed in the model above the propeller (typically 10–20 probes). The measured time histories of the pressures are decomposed in a Fourier analysis into the individual exciting orders (z , $2z$, $3z$, etc.) These can be used for comparisons among different design alternatives or as input for FEM simulations of structural vibrations.

Practical experience is that the pressure amplitude above the propeller alone is not adequate to characterize the excitation behavior of a propeller. Therefore, no generally valid limits can be stated for pressure fluctuation amplitudes. These amplitudes depend on propeller tip clearance, transmitted power, cavitation extent, etc. Nevertheless, Asmussen et al. (1998) give some guidelines: '[...] pressure amplitudes at blade frequency of 1 to 2, 2 to 8, and over 8 kPa at a point directly above the propeller can be categorized as "low", "medium" and "high",

respectively. Total vertical force fluctuations at blade frequency, integrated from pressure fluctuations, range from about 10 kN for a high-performance special-purpose ship to 1000 kN for a high-performance container vessel. For usual ship types and sizes, corresponding values lie between 100 and 300 kN. Whether these considerable excitation forces result in large vibrations depends on dynamic characteristics of the ship structure and can only be judged rationally on the basis of forced vibration analysis.'

Propellers also excite vibrations by way of unsteady propeller blade forces. These are due to the inhomogeneous wake of the ship and are transmitted via the propeller shaft into the ship. Reducing the inhomogeneity of the ship wake reduces the vibration excitation. The wake is usually determined in experiments in the model basin. In practice, the unsteady propeller forces for given wake are determined in numerical simulations.

5.6.2. Engine

Donath and Bryndum (1988) discuss in detail ship engine vibrations. Engines can be responsible for considerable vibrations. Diesel engines are far more critical in this respect than turbines. The main effects are due to the moving parts and the gas forces between pistons and cylinders. For large main engines, the vibration excitation due to horizontal and vertical total forces is typically almost zero. One often introduces the 'order' of excitation:

$$\text{order} = \frac{\text{exciting frequency}}{\text{rpm}}$$

For slow two-stroke diesels with N cylinders, the first, second, ..., N^{th} order may excite vibrations. For four-stroke diesels, half orders may also be excited. A diesel engine located on the centerplane of the ship excites (usually) vertical vibrations of first and second (i.e. with one and two times the frequency of the engine rpm) and horizontal-torsional vibrations of N^{th} order. (Also, torsional vibrations of second order may be excited.) Engines arranged off-center excite both horizontal and vertical vibrations in all integer orders. However, one can couple two symmetrically arranged engines in rpm and phase such that their excitations in horizontal or vertical vibrations cancel each other.

The natural frequencies of the ship girder change depending on the load condition (ballast, fully loaded). Nevertheless, one tries to exploit remaining off-resonance intervals for the lower natural frequencies. Besides moments around the x axis, moments around the y and z axes are excited, because mass forces of the cylinders act at different x positions. For slender, single-screw ships, the main engine has to be arranged on a slender skeg and the moments around the z axis cannot be as well absorbed as for twin-screw ships where the engines are arranged on a relatively broad flat bottom. For twin-screw ships, the moments around the x axis are more critical. Moments about the x axis appear only at orders $N, 2N, 3N, \dots$ for two-stroke engines and $0.5N, N, 1.5N, 2N, \dots$ for four-stroke engines. Fundamental natural frequencies of main

engine vibrations depend on the distribution of stiffness values and masses of the engine itself, but also to a large extent on the stiffness of adjoining structures. For large engines, particularly slow two-stroke engines, the foundation cannot be regarded as completely stiff and vibration analyses using FEM models of engine and supporting elastic structure show considerably lower natural frequencies than for infinitely rigid support (Asmussen et al. 1998).

Propeller shaft lines have to be considered together with their supporting structures. Torsional vibrations are covered by classification society rules. Axial vibrations are usually calculated by isolated models consisting of masses, springs, and damping elements. For bending vibrations, finite element computations are performed including a simple three-dimensional model of the surrounding aftbody structure. The oil film stiffness in the slide bearings for the propeller shaft and the hydrodynamic (added) mass of the propeller need to be included in the model to get realistic results. As both parameters are difficult to estimate, sensitivity analyses with parametric variations are recommended.

5.6.3. Seaway

Seaway excites a broadband of frequencies, so avoiding resonance is impossible. Ship vibrations are mainly excited by propeller and engines. The seaway excites mainly rigid-body motions such as roll, heave, and pitch. The lowest natural frequencies of vibrations of the ship hull usually lie above the significant frequencies of the seaway and are thus seldom excited. Only for very large ships, the lowest natural frequencies may become less than 1 Hz and seaway may also play a role in exciting continuous vibrations ('springing'). Slamming can induce considerable free vibrations (whipping). Studies of Germanischer Lloyd for a large LNG carrier have shown that whipping may increase bending moments (and thus longitudinal stresses) by 25%.

5.6.4. Vortex-Induced Vibrations

If unpleasant vibrations appear on board ships normally the respective frequency clearly identifies either engine or propeller as exciting source. However, for vortex-induced vibrations, the identification of the exciting sources requires considerably greater effort. In the past, the exciting source was often found only after an extensive trial-and-error approach, starting with modifications of the most likely appendages such as V-brackets, fins, sea chests, etc. This approach is inefficient, time-consuming, and costly.

Modern simulation techniques allow a more detailed insight into the physical mechanisms involving vortex shedding. They also allow rapid assessment of potential design changes. This saves time and cost for shipyard and owner. The simulations used for vortex-induced vibrations combine computational fluid dynamics (CFD) for the vortex generation and the associated vibration excitation and finite element analyses for vibration response. Based on

the simulations, many potential excitation sources can be excluded. In the end, a single final sea trial suffices to verify the excitation source in measurements and to quantify the excitation.

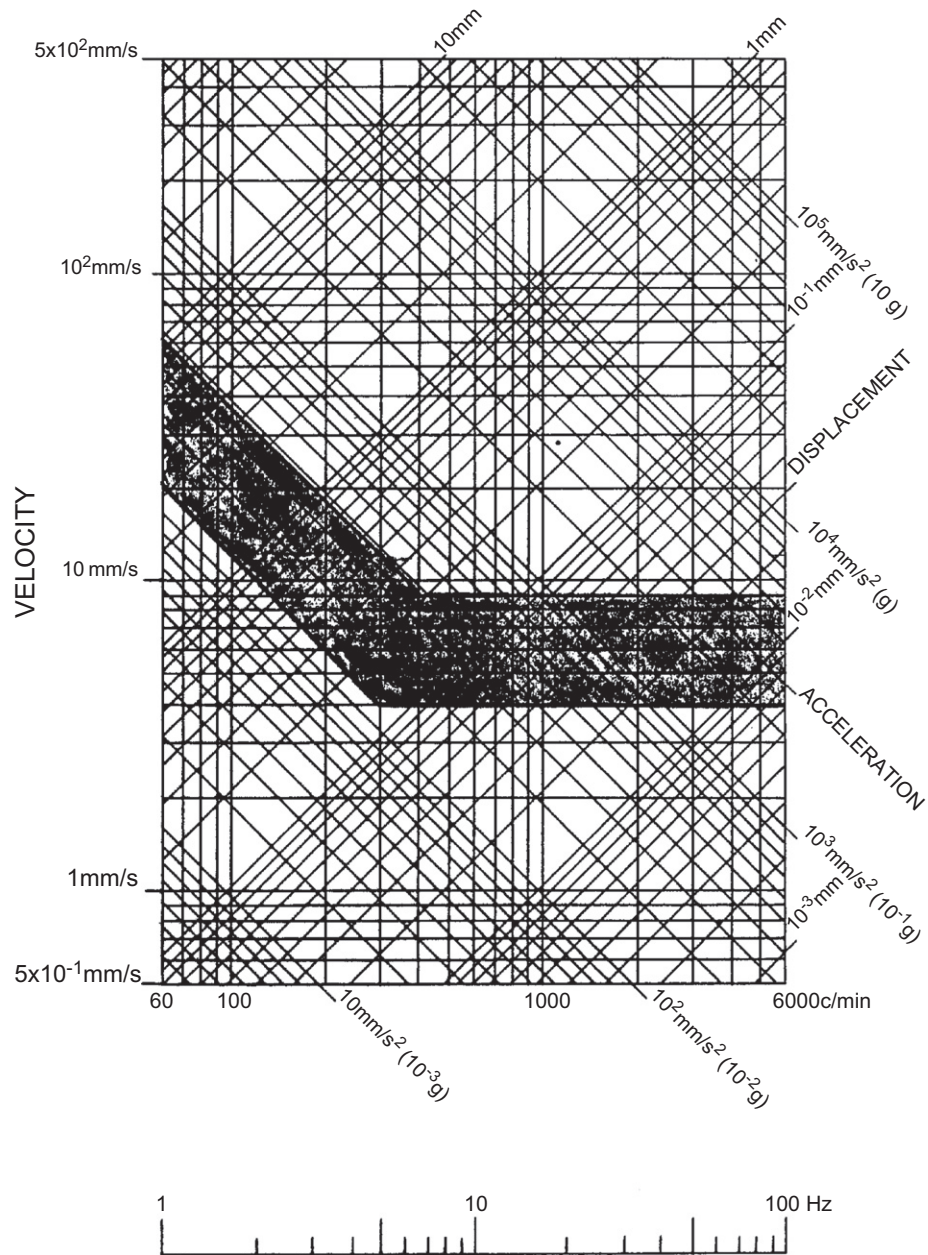
Menzel et al. (2008) describe the procedure for an actual case study:

- Sea trials reveal vibration problems. The sea trial measurements determine frequency and amplitudes.
- Comparison with engine and propeller frequencies rules out engine and propeller as exciting source.
- Three-dimensional RANSE model of ship with all appendages (and recesses like sea chests) is created and simulated in the time domain (unsteady RANSE simulation).
- Pressure histories at all appendages and recesses are analyzed to detect unsteady vortex formation with (approximately) the frequency causing the vibration problems.
- If several appendages with such critical frequency are found, finite element analyses can indicate the effect of pressure fluctuations on the structural vibration (e.g. in a given cabin). This typically narrows the source of vibration down to the appendage where large pressure amplitudes are created by the vortices, which have strong effect on a given cabin or structural part of the ship.
- Optional at this point, a dedicated sea trial may be performed with specific and detailed measurement only for this part. Increasingly, the confidence in CFD is there to avoid the added expense and time of sea trials.
- The appendage is then re-designed, typically smoothing transitions, and re-analyzed until the critical vortices disappear in the simulation.
- Then the new design is built and verified in sea trials. There is no case known where sea trials did not confirm the disappearance of the problem.

Industry experience has shown that this approach allows solving complicated vibration problems. The simulation-based approach is time- and cost-efficient, and therefore clearly superior to the traditional trial-and-error approach.

5.7. *Effect of Vibrations*

Despite careful analysis and design, vibrations on board ships cannot be avoided completely. Suitable upper limits for the effects on ship, cargo, engines, and humans can be found in various regulations and norms. Parameters employed in the evaluation of vibrations are frequency f , displacement s , vibrational velocity v and vibrational acceleration a . For harmonic vibrations, the amplitudes of s , v , and a are coupled to each other by the frequency: $v = 2\pi \cdot f \cdot s$ and $a = 2\pi \cdot f \cdot v$. Displacement and frequency thus determine also velocity and acceleration. Results of experiments or computations for vibrational analyses are often displayed in double-logarithmic form (Fig. 5.13). Above the displayed band, vibrations are no longer acceptable



$$V = s/t = 2\pi \cdot f \cdot s$$

$$\ln V = \ln 2\pi + \ln f + \ln s$$

s = DISPLACEMENT
b = ACCELERATION

$$V = b/t = b/2\pi \cdot f$$

$$\ln V = \ln b - \ln 2\pi - \ln f$$

f = FREQUENCY (Hz)
V = VELOCITY

Figure 5.13:
Double-logarithmic vibration diagram, ISO 6954

according to ISO 6954. Below the band, vibrations are uncritical. Inside the band, they are acceptable in certain conditions.

According to ISO 6954, vibration measurements on board ships shall be performed in course straight ahead, deep water and calm (at most light) sea state during usually at least 1 min (2 min if significant frequency components exist in the range below 2 Hz). These measurements are used to determine the overall frequency-weighted root mean square of the acceleration in the direction where this value is maximum. The locations where the measurements are taken are typically agreed with the ship owner. The frequency weight reflects the individual human sensitivity for different frequencies. Figure 5.14 shows the frequency weights according to ISO 6954; 10 dB (decibels) express a factor 10 for the vibration energy which is proportional to the square of the amplitudes. Example: a weight of -15 dB means that the amplitude is to be multiplied by a factor $\sqrt{10^{-15/10}} = 0.1778$.

5.7.1. Effects of Vibrations on the Ship

The main problem here is fatigue of the structural design. To estimate the life expectancy of a ship structure under dynamic load, one needs the frequencies, the vibrational amplitudes, the time span of each load group, and the Wöhler (or S–N) curve of the material. For a one-step load, i.e. a continuous harmonic load of constant amplitude, the time to crack initiation follows directly from the Wöhler curve. An ensemble of dynamic loads of different amplitudes is called a spectrum. Spectral loading increases life expectancy considerably compared to one-step loads. For reasons of fatigue strength, Germanischer Lloyd recommends limits for deflections and velocity amplitudes of vibrations in aftbodies of ships (Asmussen et al. 1998). Below 5 Hz a deflection amplitude limit of 1 mm is recommended, above 5 Hz a velocity amplitude limit of 30 mm/s. Above twice these values, premature fatigue damage is considered as probable.

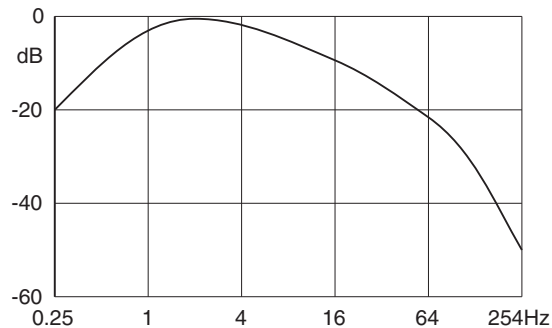


Figure 5.14:
Frequency weight according to ISO 6954

5.7.2. Effects on Engines

ISO 7919 and ISO 10816 specify that engines and connected aggregates should generally not be subject to vibrations exceeding any of the following limits: 0.71 mm deflection amplitude; 14 mm/s velocity amplitude; 0.7 g acceleration amplitude. For rudder gear rooms and bow thruster rooms, we accept velocity amplitudes approximately twice as high and acceleration amplitudes approximately four times as high. Classification societies have also incorporated these limits in their rules.

5.7.3. Effects of Vibrations on Humans

The most frequent cause of re-design due to vibration problems concerns effects on humans. Different standards exist for vibrations in ship rooms. ISO 6954 covers vibrations on merchant ships and its effects on humans. ISO 6954 gives values for the overall frequency-weighted root mean square acceleration and velocity, above which adverse comments are probable (Table 5.5). Below half these values, adverse comments are not probable. The zone between upper and lower values reflects the shipboard vibration environment commonly experienced and accepted. The values are determined over the frequency range from 1 Hz to 80 Hz. The limits are different for categories A (e.g. passenger cabins), B (e.g. crew rooms), and C (e.g. operational rooms).

For harmonic oscillations, root mean square σ and maximum amplitude a are coupled by $a = \sqrt{2} \cdot \sigma$.

Classification societies have introduced ‘comfort classification’ with respect to vibration levels (e.g. Det norske Veritas, Table 5.6): for comfort rating number 1, 2, or 3, the velocity amplitudes are considered separately for all appearing frequencies. For each individual frequency and each measured location, limit values may not be exceeded. Only for frequencies below 5 Hz can the measured velocity amplitude be reduced by the ratio of actual frequency to 5 Hz.

ISO 2631 also concerns the effect of mechanical vibrations on humans, at low frequencies 0.1–0.5 Hz (ship motion sickness) and higher frequencies 0.5–80 Hz (health, comfort). Important parameters are frequency, direction of vibration, and the form in which the vibrations enter the human body. We thus perceive vibrations differently depending on whether

Table 5.5: Values of overall frequency-weighted r.m.s. values for acceleration and velocity, above which adverse comments are probable, ISO 6954

A		B		C	
143 mm/s ²	4 mm/s	214 mm/s ²	6 mm/s	286 mm/s ²	8 mm/s

Table 5.6: Velocity amplitude limits (mm/s) for three comfort classes following Det norske Veritas

Comfort rating number	1	2	3
High speed and light craft			
– passenger localities, navigation bridge, offices	2.0	3.5	5.0
– control rooms	3.0	4.5	6.0
Passenger ships			
– top-grade cabins	1.5	2.0	2.5
– standard cabins, public spaces	1.5	2.5	4.0
– open deck recreation	2.5	3.5	5.0
Yacht (owner and guest areas)			
– accommodation on sea/in port	1.0/0.5	2.0/1.0	3.0/2.0
– outdoor recreation areas	2.0/0.5	3.0/1.0	4.0/2.0
– navigation bridge	1.5	2.5	4.0
Cargo ships			
– cabins, mess, recreation rooms, offices, bridge	2.5	3.5	5.0
– control rooms, work places	3.5	4.5	6.0

they enter the body via our feet, our hands, or our buttocks. The relevant frequency range lies approximately between 1 and 100 Hz. For vibrations below 1 Hz, the body reacts with motion sickness (nausea). Objective criteria cannot be formulated as individual people react very differently to vibrations. This may be due to different natural frequencies of individual body parts. Subjective criteria are comfort (feeling well), ability to perform, and health. ISO 2631 classifies the direction of vibrations in a body-fixed coordinate system (Fig. 5.15), and gives admissible vibrational accelerations (e.g. Fig. 5.16). The curves have the duration of the effect as a parameter.

Table 5.7 lists typical natural frequencies of body parts and symptoms for vertical vibrational exciting of a sitting human with amplitude at tolerance threshold.

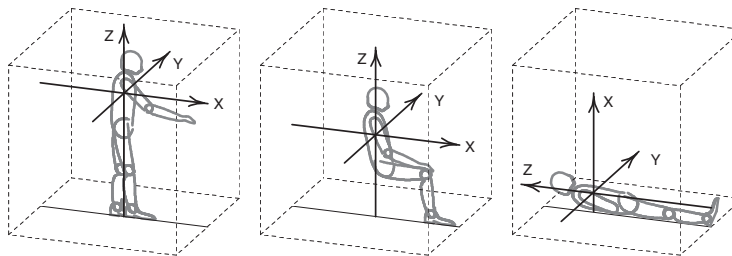


Figure 5.15:
Vibration directions with reference to human body

To obtain

"exposure limits" :multiply acceleration values by 2 (6 dB higher) ,

"reduced comfort boundary " :divide acceleration values by 3,15 (10 dB lower)

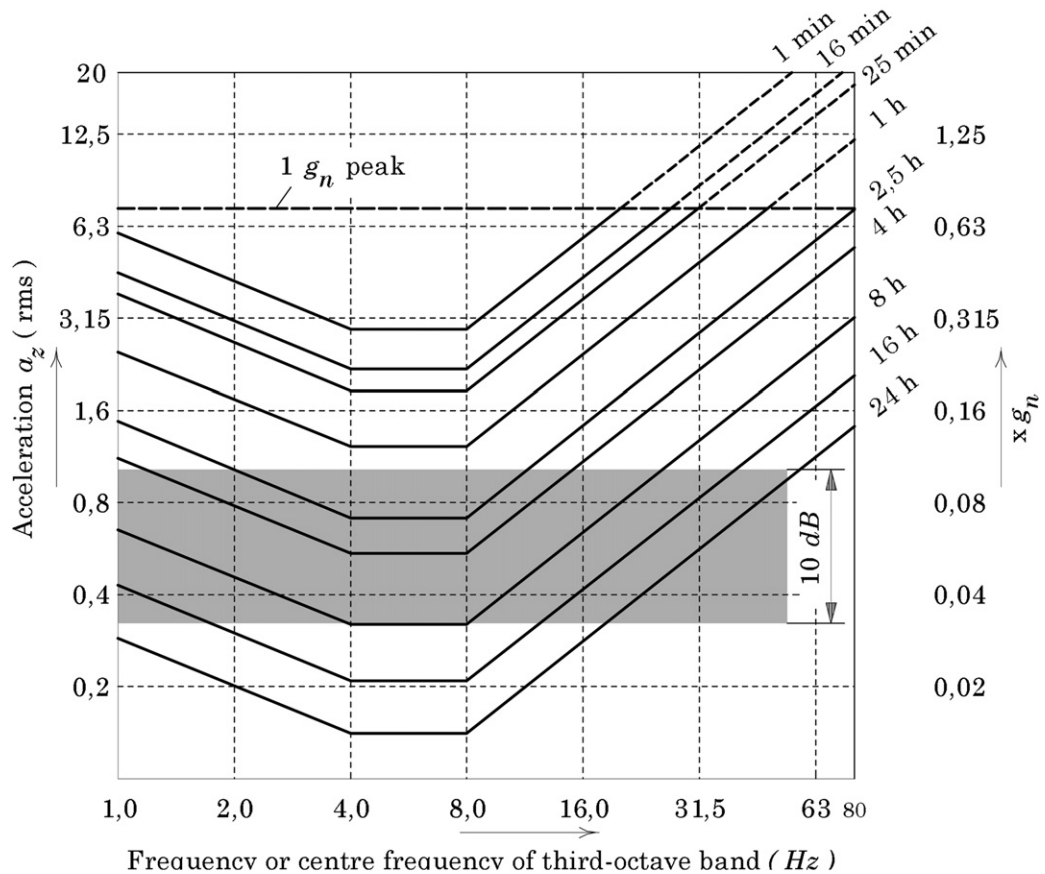


Figure 5.16:

Threshold values in the direction of the body's longitudinal axis, ISO 2631

Table 5.7: Effect of vibrations on sitting human

Body part	Effect of threshold vibration	Natural frequency
Brain	General discomfort, nausea	4.5–9 Hz
Head	Difficulty to speak	13–20 Hz
Chest	Pain in chest, breathing difficulties	4–8 Hz
Back	Back pain	8–12 Hz
Intestines	Urge to release feces	10.5–16 Hz
Bladder	Urge to release urine	10–18 Hz
Legs	Increased muscle tension	13–20 Hz
Abdomen	Abdominal pain	4.5–10 Hz